GRAFTING ON MALEIC ANHYDRIDE-GRAFTED POLY(BUTYLENE SUCCINATE) VIA ONE-STEP REACTIVE GRAFTING PROCESS AND COMPATIBILIZATION ON THE POLY(BUTYLENE SUCCINATE) NANOCOMPOSITES

Z.A Mohd Ishak[1,2,]*, W.S. Chow[1,2], Y.J. Phua[1,2]

[1]*Cluster for Polymer Composites, Engineering and Technology Research Platform, Engineering Campus, Universiti Sains Malaysia, 14300 Nibong Tebal, Penang, Malaysia.*
[2]*School of Materials and Mineral Resources Engineering,*

Engineering Campus, Universiti Sains Malaysia, 14300 Nibong Tebal, Penang, Malaysia
**Corresponding Author: Prof. Dr. Zainal Arifin Mohd Ishak (zarifin@eng.usm.my, zarifin.ishak@gmail.com)*

Keywords: Poly(butylene succinate), Nanocomposites, Grafting, Compatibilization

Abstract
Maleic anhydride-grafted poly(butylene succinate) (PBS-g-MA) was prepared via a one-step reactive grafting process, and characterized by Fourier transform infrared (FTIR) spectroscopy and nuclear magnetic resonance (NMR) spectroscopy. Then, nanocomposites were produced between PBS and organo-montmorillonite (OMMT), by using PBS-g-MA as a compatibilizer. Tensile and flexural properties of nanocomposites were enhanced after compatibilization, due to better filler dispersion as revealed through X-ray diffraction (XRD) and transmission electron microscopy (TEM). From the differential scanning calorimetry (DSC) analysis, it is understood that the increment in crystallinity could also be partially responsible for the increase in mechanical properties. However, the presence of compatibilizer slightly increased the biodegradability of the material.

1 Introduction

Poly(butylene succinate) (PBS) is one of the most promising biodegradable polyesters with many desirable properties including biodegradability, melt processability, thermal and chemical resistance. Conversely, PBS posses some drawbacks such as softness, low melt viscosity for further processing, poor tensile and gas-barrier properties [1]. In particular, these drawbacks can be overcome by the addition of organo-montmorillonite (OMMT) to form a nanocomposite. Numerous researchers reported on the enhanced strength and modulus [1], gas barrier [2] and flame retardant properties [3] after the incorporation of OMMT into various polymer matrices. In our previous work, the enhanced mechanical and rheological properties of biodegradable PBS/OMMT nanocomposites have been reported [4-5]. However, there is still room for improvement to produce PBS/OMMT nanocomposites with a better performance, by improving the filler-matrix interactions and filler dispersion.

Maleic anhydride (MA) grafted polymers has been widely used as compatibilizer in nanocomposite system by reason of their polar functional group that will facilitate the OMMT dispersion. Hence, MA grafted PBS (PBS-g-MA) was produced via a one-step reactive

grafting process. Fourier transform infrared (FTIR) spectroscopy and nuclear magnetic resonance (NMR) spectroscopy provide the information on the grafting mechanism. To date, PBS-g-MA is not commercially available and has limited literature reported on this material. The main objective of this study is to investigate the effects PBS-g-MA as compatibilizer on the mechanical, morphological, thermal and biodegradation properties of PBS/OMMT nanocomposites.

2 Experimental

2.1 Materials

PBS (Bionolle #1020) with melting temperature of 115°C was obtained from Showa Highpolymer Co., Ltd., Japan. OMMT (Nanomer® I.30TC) was supplied by Nanocor Inc, USA. Dicumyl peroxide (DCP) (Aldrich Luperox®) from Sigma-Aldrich Inc, USA was used as initiator. MA (M_w = 98.06) was obtained from R&M II Chemicals, USA.

2.2 Synthesis of PBS-g-MA

PBS (100phr), MA (10phr) and DCP (1.5phr) were physically premixed and blended in an internal mixer (Haake Polydrive R600, Germany) at 135°C for 7 min. Subsequently, the PBS-g-MA was purified by using methanol. Then, the obtained PBS-g-MA was characterized by using Fourier transform infrared (FTIR) spectroscopy at ambient temperature by using Perkin-Elmer Spectrum One FT-IR Spectrometer, USA, at scanning wavelength of 4000-400 cm^{-1} with 32 scanning times. Nuclear Magnetic Resonance (NMR) Spectroscopy were conducted in deuterated chloroform ($CDCl_3$) solution under ambient temperature on a Bruker Avance 300 MHz spectrometer (Germany). Tetramethylsimane (TMS) was applied as internal chemical shift standard. Two-dimensional correlation spectroscopy (COSY) was also recorded. Degree of grafting for PBS-g-MA was determined through titration process by using potassium hydroxide (KOH) as below:

$$G_d(\%) = \frac{N(V_1 - V_o) \times 98.06}{2 \times W \times 1000} \times 100\% \quad (1)$$

where N is the concentration of KOH (M), W is the weight of sample (g), V_o is the volume of KOH (ml) for the blank solution and V_1 is the volume of KOH (ml) for the titration of PBS-g-MA solution. The molecular weight of PBS was measured by GPC analysis. GPC analysis was performed at 40°C on an Agilent Technologies 1200 Series GPC system (USA) equipped with a refractive index detector (RID) and SHODEX K-806M and SHODEX K-802 columns.

2.3 Preparation of nanocomposites

Melt-mixing of PBS with OMMT was performed using an internal mixer (Haake PolyDrive R600, Germany) for 5 min at 135 ℃ and a rotary speed of 50rpm. Three different compounds were prepared, which are the neat PBS, uncompatibilized nanocomposite filled with 2wt% OMMT, as well as compatibilized nanocomposite filled with 2 wt% OMMT and 5wt% PBS-g-MA as compatibilizer. The compound was then molded on a compression molding machine (GT 7014-A30C, Taiwan) at 135 ℃ and 3 min.

2.4 Characterizations of nanocomposites

Mechanical tests were performed using an Instron 3366 machine (USA) at ambient temperature. Tensile test was carried out according to ASTM D638-03 (Type IV) with gauge length of 50mm and cross-head speed of 5mm/min. Flexural test (three-point bending) was performed according to ASTM D790-03 with a support span length of 50mm and cross-head speed of 5mm/min.

The tensile-fractured surface of the samples was examined under a field-emission scanning electron microscope (FESEM) (Zeiss LEO Supra 35VP, Germany). Prior to the observations, the sample was sputter-coated with a thin layer of gold to avoid electrical charging during examination. XRD analysis was carried out on the nanocomposites with PANalytical X'pert Pro Mrd PW2040 XRD diffractometer in a scan range from 2^o-10^o and 2.0^o/min scanning rate. The morphologies of the nanocomposite samples were observed using an Energy Filter Transmission Microscope (EFTEM) (Zeiss Libra 120, Netherlands) operated at 200 kV. The ultrathin sections of sample with the thickness 70–80 nm were prepared via ultramicrotomy technique using Reichert Ultramicrotome Supernova.

DSC analysis was carried out using Perkin-Elmer DSC-6 (USA) in nitrogen atmosphere. Sample was heated from 30^oC to 150^oC at a heating rate of 10^oC/min. The sample was cooled from 150^oC to 30^oC at a same heating rate. Second heating was performed from 30^oC to 150^oC. Finally, it is cooled to room temperature.

Soil burial test was conducted by burying the samples in natural organic humus compost soil. Each specimen was buried in the compost soil and incubated at environmental temperature of 30±2 ℃ and 60-70% relative humidity. Water was supplied constantly to keep the compost soil humid. Each specimen was dug out periodically, washed with distilled water and dried to a constant weight at 60 ^{o}C in a vacuum oven. The percentage of weight loss was measured using an electronic balance.

The natural weathering test was carried out according to ASTM D1435. Specimens in dumbbell shapes were attached to a stationary rack at an inclination angle of 45 ° facing to south. This test was conducted in Universiti Sains Malaysia, Nibong Tebal, Penang, Malaysia (latitude 5° 08' N, longitude 100° 29' E) for 6 months from January 2011 to June 2011. During the natural weathering test, the specimens were collected periodically, washed with distilled water and dried to a constant weight at 60 ^{o}C in a vacuum oven before weighing.

3 Results and Discussion

3.1 Characterizations of PBS-g-MA

After the grafting process, PBS-g-MA with 4.84% degree of grafting was obtained. The degree of grafting of PBS-g-MA that obtained in this work is appeared to be higher than that of the conventional grafted polymers such as MA grafted PP, with the degree of grafting ranged between 0.5-1.2% [6]. The weight-average molecular weight (M_w) of PBS-g-MA is 24260 g/mol, while the M_w of the neat PBS before grafting process is 1.4 x 10^5 g/mol. Thus, this shows that as the PBS is grafted with MA, the molecular weight is reduced as a result from chain degradation via the beta-scission reaction

The FTIR spectroscopy was presented in Figure 1, and the PBS-g-MA was labeled as C2. The peak at 917 cm^{-1} corresponds to the −C−OH bending in the carboxylic acid groups of PBS. The bands at 1044-1046 cm^{-1} were due to −O−C−C− stretching vibrations in PBS. Peaks in the range of 1144-1264 cm^{-1} resulted from the stretching of the −C−O−C− group in the ester linkages of PBS. The band at the 1710-1713 cm^{-1} region was attributed to the C=O stretching vibrations of ester groups in PBS. Meanwhile, the peaks at 1330 cm^{-1} and 2945 cm^{-1} were assigned to the symmetric and asymmetric deformational vibrations of $-CH_2-$ groups in the PBS main chains, respectively [7]. There is a clear signal at the transmittance bands of

1780 cm^{-1} and 1849 cm^{-1} in the PBS-g-MA, while were absent in the neat PBS. These bands are assigned to the symmetric (1780 cm^{-1}) and asymmetric (1849 cm^{-1}) stretching of C=O bonds for the succinic anhydride groups. Furthermore, an additional band at 3058 cm^{-1} was found in PBS-g-MA and neat MA, ascribed to the $=CH_2$ vibration in the cyclic MA. This confirms the grafting of MA onto PBS.

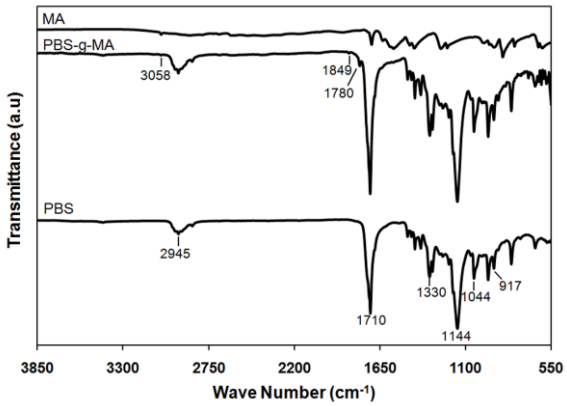

Figure 1. FTIR spectra of PBS and PBS-g-MA

The ^{1}H-NMR spectra of neat PBS and PBS-g-MA are shown in Figure 2. The signal of at 2.55 ppm was associated with the methylene protons (H_a) in the succinic moiety. The resonances at 4.05 and 1.64 ppm were respectively assigned to the methylene protons α (H_b) and β (H_c) in the 1,4-butanediol unit. An additional signal is observed in the PBS-g-MA spectra at approximate 3.7 ppm region, which is related to the resonance of the methane proton formed due to the grafting of MA [8]. This supports the evidence that MA is attached to the polymer chains after the reactive grafting process. The 2D COSY ^{1}H-NMR spectra (Figure 3) provides additional information on the grafting mechanism. The off-diagonal peaks or cross correlated peaks show a single coupling interaction between the methine proton of the anhydride with protons of the α carbon atom ($H_{b'}$) in the 1,4-butanediol unit (Figure 3b). This result suggests that the grafting reaction take place at the diol unit of PBS.

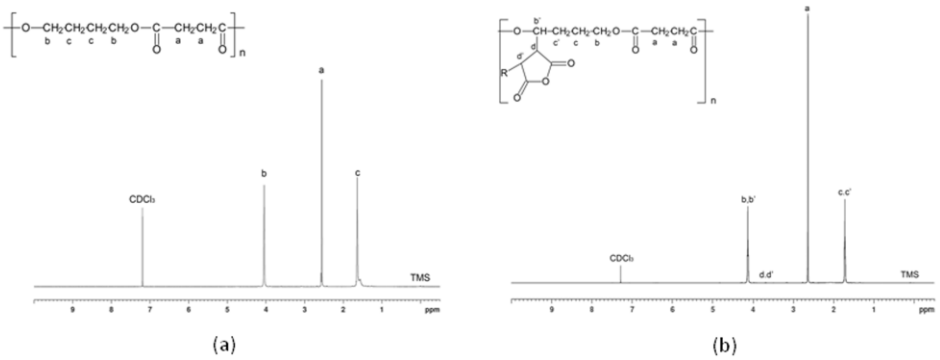

Figure 2. ^{1}H-NMR spectra of (a) neat PBS and (b) PBS-g-MA

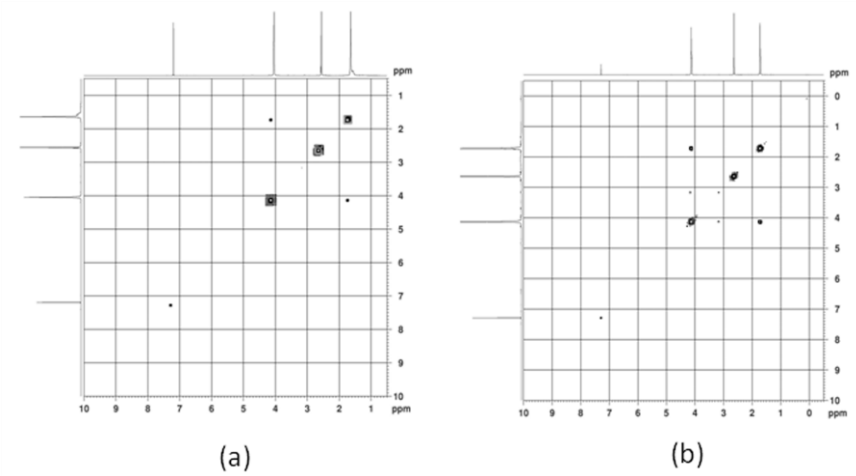

Figure 3. 2D COSY ^{1}H-NMR spectra of (a) neat PBS and (b) PBS-g-MA

3.2 Characterizations of PBS nanocomposites

3.2.1 Mechanical properties

Table 1 shows that the strength and modulus improved after compatibilization. The PBS-g-MA may react with the hydroxyl groups of OMMT on one side, and with the carboxylic groups of the PBS-g-MA diffused matrix polymer on the other side. This consequently improved the filler-matrix interaction, meanwhile, enhanced the filler dispersion through the intercalation of anhydride groups between the OMMT galleries. The increase in modulus may also relate to the higher stiffness of PBS-g-MA due to the presence of cyclic structure in the anhydride groups. However, the incorporation of PBS-g-MA does not show significant effect on the elongation at break.

Properties	**Compound**		
	PBS	**Uncompatibilized**	**Compatibilized**
Tensile			
Strength (MPa)	32.6 ±2.7	33.6 ±1.2	37.1 ±1.3
Modulus (MPa)	589 ±6.8	631 ±9.1	650 ±7.2
Elongation at break (%)	10.9 ±2.6	12.9 ±2.4	12.5 ±1.8
Flexural			
Strength (MPa)	33.3 ±1.9	36.1 ±0.91	38.3 ±0.18
Modulus (MPa)	570 ±14	619 ±11	626 ±3.9

Table 1. Mechanical properties of PBS and the nanocomposites

3.2.2 Morphological properties

Figure 4 displays the tensile fractured surface of PBS and its nanocomposites. PBS exhibits a semi-ductile fracture behavior, indicated by the relatively smooth and clear surface with fibrils that formed a web-like structure. Fractured surface of uncompatibilized nanocomposites reveals a reduction in the fibrillation of PBS, due to the stiffening effect after OMMT addition. At certain area, distinct phase separation between the OMMT platelets and the PBS matrix is noticeable due to poor filler-matrix interactions. The compatibilized nanocomposite shows no clear filler delamination from the PBS matrix, confirms the improved filler-matrix interactions in the nanocomposites after compatibilization.

TEM images of the compatibilized and uncompatibilized nanocomposites are displayed in Figure 5. A mixed region of intercalated clay platelet stacks, and individual exfoliated platelets are present in the uncompatibilized nanocomposites. After compatibilization using PBS-g-MA, a higher degree of intercalated and exfoliated clay platelets was obtained, as presented in Figure 5b. The TEM images have provided a direct

visualization of the improved dispersion of OMMT in PBS matrix, which is in good agreement with observed mechanical properties.

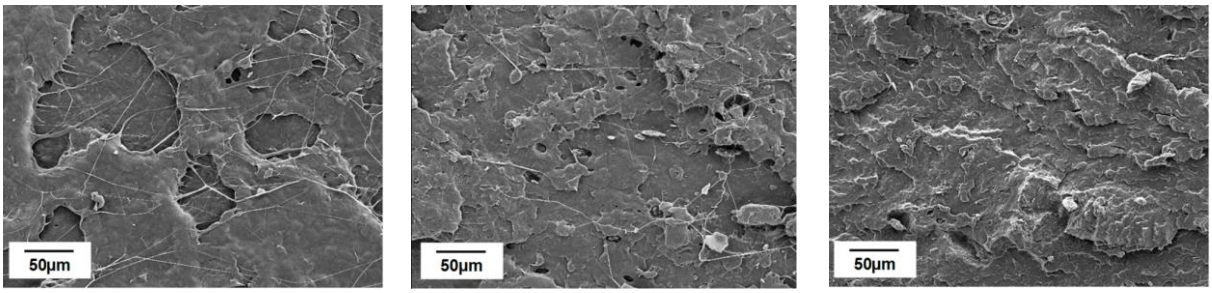

(a) (b) (c)

Figure 4. SEM micrographs of (a) neat PBS, (b) uncompatibilized and (c) compatibilized nanocomposite

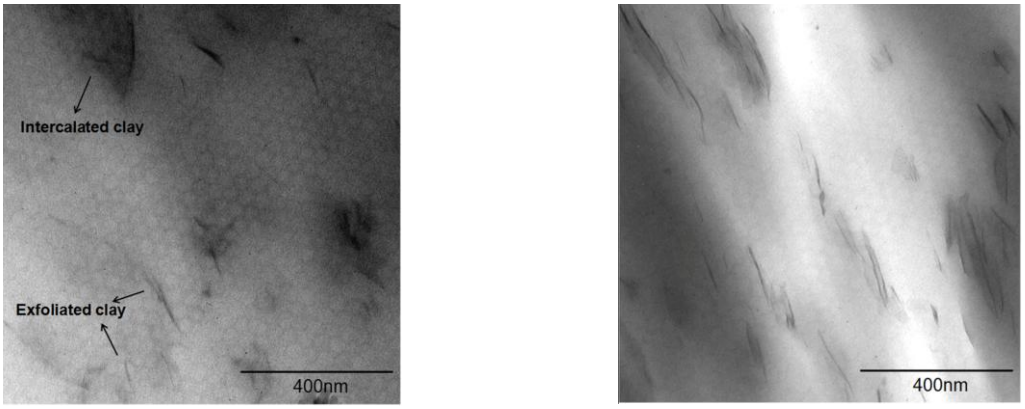

(a) (b)

Figure 5. TEM images of (a) uncompatibilized and (b) compatibilized nanocomposite

Figure 6 presents the XRD patterns of OMMT and the nanocomposites. A clear peak showing the interlayer spacing associated with the d_{001} plane of MMT was observed. The XRD spectrum of OMMT exhibits a broad intense peak at $2\theta=3.17°$, corresponding to a d_{001} spacing of 2.79 nm. It is clear that the peaks tend to broaden and shift toward a lower value of 2θ after the formation of nanocomposites, suggesting the formation of intercalated and exfoliated structures in the nanocomposites [9]. The XRD patterns of uncompatibilized and compatibilized nanocomposites reveal the diffraction peaks at $2\theta=2.46°$ and 2.23 °, corresponding to the d_{001} spacing of 3.59nm and 3.95nm, respectively. Hence, Addition of PBS-g-MA into the nanocomposites is proven to further facilitate the expansion of gallery space between the organoclay layers.

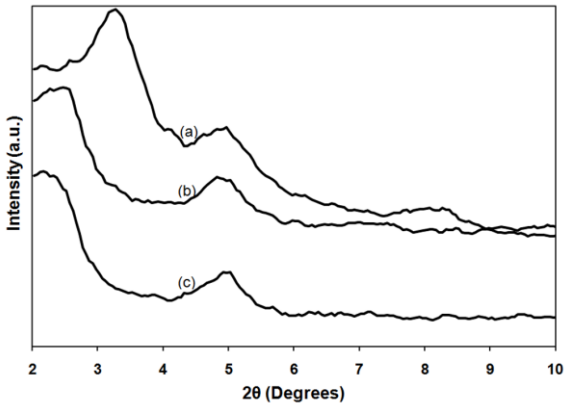

Figure 6. TEM images of (a) OMMT, (b) uncompatibilized and (c) compatibilized nanocomposite

3.2.3 Thermal properties

Two distinct peaks were found in the heating scan (Figure 7a), where the low endotherm is corresponds to the melting of the original crystallites; and the high endotherm is corresponds to the melting of the recrystallized one [4]. From Table 2, it is noted that the incorporation of PBS-g-MA slightly increased the melting temperature at the low endotherm ($T_{m,x}$). This is assigned to the interfacial chemical reaction between the MA group in PBS-g-MA and carbonyl group in PBS, as well as the increased degree of crystallinity after compatibilization. This shows that PBS-g-MA acts as a heterogeneous nucleating agent, creating nucleating sites for the crystallization process to occur. The reduction in crystallization temperature (T_c) after compatibilization is attributed to slower crystal growth generated by the interactions between PBS and PBS-g-MA.

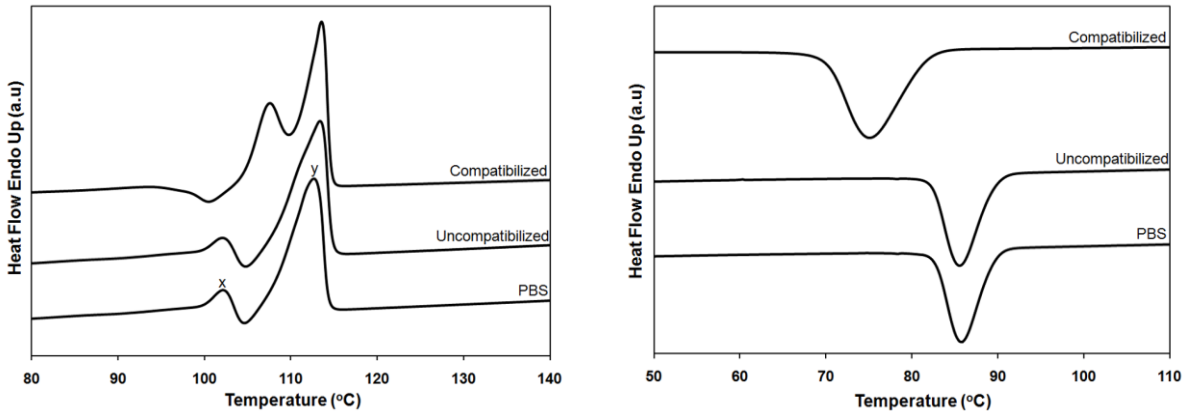

Figure 7. DSC (a) heating and (b) cooling scans of PBS and the nanocomposites

Compound	$T_{m,x}$ (°C)	$T_{m,y}$ (°C)	T_c (°C)	χ_c (%)
PBS	102.2	112.4	85.9	57.6
Uncompatibilized	102.1	113.4	85.6	55.7
Compatibilized	107.4	113.6	82.1	65.9

Table 2. DSC results of PBS and the nanocomposites

3.2.4 Degradation analysis

Figure 8 presents the weight loss of PBS and the nanocomposites along 180 days of soil burial and natural weathering. At the initial stage, the weight loss increased rapidly as a function of exposure time, due to the degradation of low molecular weight fragments and exposed end groups in PBS. The weight loss was then attained a steady state after 60 to 90 days. The weight loss of PBS nanocomposites is lower as compared to the neat PBS, owing to the improvement of the barrier properties after addition of clay. This consequently restricted the penetration of microorganism through the material. Addition of PBS-g-MA slightly increased the weight loss of the material, reveals a higher biodegradability in the compatibilized nanocomposites. It is believed that the low molecular weight of PBS-g-MA is responsible in enhancing the biodegradability. In addition, the moisture in the environment penetrated into the nanocomposites, subsequently reacted with the MA groups in PBS-g-MA to form succinic acid through hydrolysis process. This acid group accelerated the chain scission of PBS, resulting in a higher biodegradability.

4 Conclusions

The PBS-g-MA was successfully synthesized. The addition of PBS-g-MA into PBS nanocomposite as a compatibilizer was found to enhance the mechanical properties and

biodegradability. Better OMMT dispersion was formed after compatibilization as shown in the morphological properties. Furthermore, PBS-g-MA acts as a heterogeneous nucleating agent that caused the increase in degree of crystallinity.

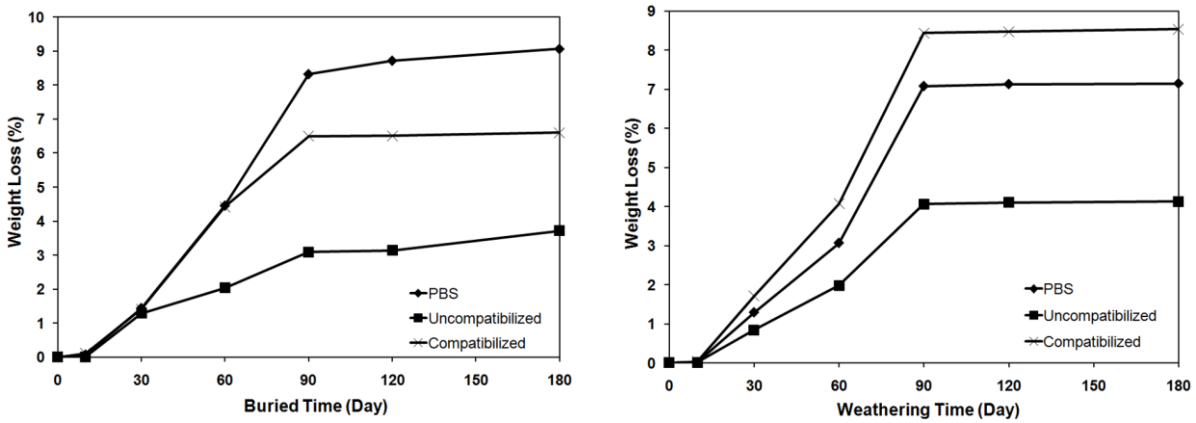

(a) (b)

Figure 7. Weight loss after 180 days exposure to (a) soil burial and (b) natural weathering

References

[1] Okamoto K., Ray S.S., Okamoto M. New poly(butylene succinate)/layered silicate nanocomposites. II. Effect of organically modified layered silicates on structure, properties, melt rheology, and biodegradability. Journal of Polymer Science: Part B: Polymer Physics, **41**, p.p. 3160-3172 (2003).

[2] Yano K., Usuki A., Okada A., Kurauchi T., Kamigaito O. Synthesis and properties of polyimide–clay hybrid. Journal of Polymer Science: Part A: Polymer Chemistry, **31**, p.p. 2493-2498 (1993).

[3] Gilman J.W., Jackson C.L., Morgan A.B., Jr R.H., Manias E., Giannelis E.P., Wuthenow M., Hilton D., Phillips S.H. Flammability properties of polymer-layered-silicate nanocomposites. Polypropylene and polystyrene nanocomposites. Chemistry of Materials, **12**, p.p. 1866-1873 (2000).

[4] Phua Y.J., Chow W.S., Mohd Ishak Z.A. Poly(butylene succinate)/ organo-montmorillonite nanocomposites: Effects of the organoclay content on mechanical, thermal, and moisture absorption properties. Journal of Thermoplastic Composite Materials, **24**, p.p. 133-151 (2010).

[5] Phua Y.J., Chow W.S., Mohd Ishak Z.A. Mechanical properties and structure development in poly(butylene succinate)/organo-montmorillonite nanocomposites under uniaxial cold rolling. eXPRESS Polymer Letters, **5**, p.p. 93-103 (2011).

[6] Kim H.S., Lee B.H., Choi S.W., Kim S., Kim H.J. The effect of types of maleic anhydride-grafted polypropylene (MAPP) on the interfacial adhesion properties of bio-flour-filled polypropylene composites. Composites Part A**:** Applied Science and Manufacturing, **38**, p.p. 1473-1482 (2007).

[7] Phua Y.J., Chow W.S., Mohd Ishak Z.A. The hydrolytic effect of moisture and hygrothermal aging on poly(butylene succinate)/organo-montmorillonite nanocomposites. Polymer Degradation and Stability, **96**, p.p. 1194-1203 (2011).

[8] Mani R., Bhattacharya M., Tang J. Functionalization of polyesters with maleic anhydride by reactive extrusion. Journal of Polymer Science: Part B: Polymer Chemistry, **37**, p.p. 1693-1702 (1999).

[9] Parija S., Nayak S.K., Verma S.K., Tripathy S.S. Studies on physico-mechanical properties and thermal characteristics of polypropylene/layered silicate nanocomposites. Polymer Composites, **25**, p.p. 646-652 (2004).